# The influence of muscle activity on head-neck response during impact

*Citation for published version (APA):*
Horst, van der, M. J., Thunnissen, J. G. M., Happee, R., Haaster, van, R. M. H. P., & Wismans, J. S. H. M. (1997). The influence of muscle activity on head-neck response during impact. In P. Prasad (Ed.), *41st Stapp car crash conference proceedings : November 13-14, 1997, Orlando, Florida* (pp. 487-507). [973346] (SAE Technical Paper; Vol. 973346). Society of Automotive Engineers (SAE). https://doi.org/10.4271/973346

*DOI:*
10.4271/973346

*Document status and date:*
Published: 01/01/1997

*Document Version:*
Publisher's PDF, also known as Version of Record (includes final page, issue and volume numbers)

973346

# The Influence of Muscle Activity on Head-Neck Response During Impact

**M. J. van der Horst**
Eindhoven University of Technology and Maastricht University

**J. G. M. Thunnissen and R. Happee**
TNO Crash Safety Research Centre and Eindhoven University of Technoloy

**R. M. H. P. van Haaster**
TNO Crash Safety Research Centre

**J. S. H. M. Wismans**
TNO Crash Safety Research Centre and Eindhoven University of Technology



## ABSTRACT

In the past, muscle activation has been identified as having an important effect on the head-neck response in dynamic conditions. However, this claim has been largely based on global observations, and not by accurate analysis. In this study, the influence of muscle activation on the head-neck response is investigated by mathematical modeling. The detailed mathematical head-neck model presented by De Jager is improved by modeling the neck muscles in more detail. A multi-segment muscle description is applied in which the muscles curve around the vertebrae, resulting in realistic muscle lines of action. The model is validated with human volunteer responses to frontal and lateral impact at several severities. The model response with maximum muscle activation to high severity frontal and lateral impacts agrees well with volunteer responses, whereas a submaximum activation level or a larger reflex delay provides better results for the low severity impacts. The simulations show that muscle contraction has a large influence on the head-neck response.

## INTRODUCTION

Neck injuries occur frequently in car accidents resulting in human suffering with high social costs. This is due to a high injury incidence and a considerable risk of long-term impairment. The mechanisms causing injuries to the neck are not fully understood as the neck is an anatomically and mechanically complex structure. Both experimental research and mathematical modeling may aid in the understanding of neck injuries.

Biomechanical models with increasing complexity are presented in the literature. However, only a few models incorporate neck muscles as separate structural elements [1,2][a]. Despite good intentions, these models describe the activity of the muscles using passive components (e.g. springs and dampers). A very simple two-pivot head-neck model with muscles that can be activated individually was presented by Happee and Thunnissen [3]. The muscle activation force was modeled by using the non-linear functions of Hill [4,5]. A detailed model of the head-neck system with muscles was presented by De Jager [6]. The model was based on the model of Deng and Goldsmith [2], and comprises rigid body head and vertebrae connected through linear viscoelastic discs, nonlinear viscoelastic ligaments, facet joints, and Hill-type muscles. The model was validated for 7g lateral and 15g frontal volunteer experiments [7,8]. The lateral experiments were described very well, but the response was too flexible for the frontal experiments. This lack was mainly attributed to the incapability of the muscle elements to curve around the vertebrae: this appeared to be a particular problem in the case of large neck rotations. Despite this shortcoming, the simulations showed that the influence of activated muscles on the head-neck response is large, as demonstrated earlier by Williams and Belytschko [9] and by biological

---

[a] Numbers in brackets designate references at end of paper.

experiments [10,11,12,13,14], even with accelerations up to 15g.

Muscular activity has been studied in biological experiments. However, presumably due to technical problems, results that quantify the timing and level of muscular activation have not been published to the best knowledge of the authors. Therefore, mathematical modeling is considered a more feasible approach for studying the role of muscular activation in impact conditions.

OBJECTIVE - The objective of our study is to investigate the influence of muscle activation on the head-neck response by modeling. An improved mathematical head-neck model based on De Jager's model [6,15] will be validated with human responses to frontal and lateral impact at several impact severities (G levels).

METHOD - The original detailed multi-pivot head-neck model of De Jager [6,15] is adapted by improving the muscle geometry, including more muscles, and dividing the muscles into a number of segments, allowing the muscles to curve around the vertebrae during neck bending. A pilot study of this new head-neck model, which will be named "Curved Muscle Neck" model (CMN model) can be found in [16]. This CMN model is validated using the human volunteer head-neck responses subjected to 15g frontal and 7g lateral HYGE sled experiments performed at the Naval Biodynamics Laboratory (NBDL) [17]. To study the effect of muscle behavior on the head-neck response, both active and passive muscle behavior is simulated, i.e. with and without muscle activation. The CMN model is also verified for frontal impacts at lower G levels (12g, 10g, 8g, 6g, 3g). Finally, a limited parametric study in which the activation level and reflex delay of the muscles are varied is conducted to investigate the influence of muscle activation.

## MODEL DESCRIPTION

The detailed model comprises nine rigid bodies, representing the head, the seven cervical vertebrae, and the first thoracic vertebra (T1). Ellipsoids represent the skull and the vertebrae with spinous and transverse processes, and articular facet surfaces. The bodies are connected through three-dimensional linear viscoelastic discs, two-dimensional nonlinear viscoelastic ligaments, frictionless facet joints (ellipsoid contacts), and contractile Hill-type muscles. For a detailed description of the elements, the reader is referred to [15]. The model is implemented in the integrated multibody/finite-element package MADYMO 5.2.1 [18].

MUSCLE GEOMETRY - In the original model, the muscles are modeled as straight line elements connecting origin to insertion, consequently, the muscles could not follow the curvature of the neck, resulting in too large head and neck rotations [6,15]. In the CMN model, intermediate frictionless sliding points through which the muscles pass simulate the curving of the muscles around the vertebrae during neck bending (see Figure 1). This curved musculature is modeled by a chain of connected muscle segments [18]. The muscular tension force is based on the active state, and total lengthening and lengthening velocity of the muscle.

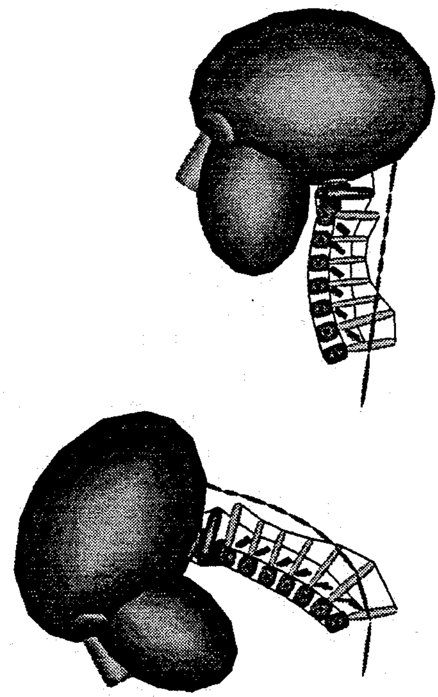

Figure 1: Path of a multi-segment muscle in initial and flexed position. Only one part of the semispinalis capitis is shown to clarify muscle curvature. The intermediate sliding points are attached to the vertebrae.

It is generally assumed that in the human body the dorsal muscles generate the largest torque at T1 level and that this torque decreases in the direction of the head. According to Happee and Thunnissen [19], the resulting maximum torques at T1-level for the model should be around 100 Nm for the extensor muscles and 44 Nm for the flexor muscles. The maximum isometric torques of the original model deviate considerably from the expected behavior. Therefore, compared to the original model, more muscles are included and muscle geometry is improved (see Appendix). Some muscles are represented by more than one muscle element to account for different points of attachment of the muscle group [20]. Maximum torque and torque distribution is improved for extension (see Figure 2) and flexion compared with the original model.

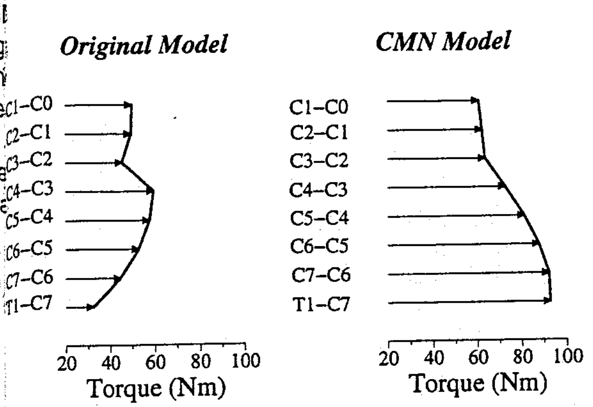


Figure 2: Comparison of extension torques in initial position due to maximum isometric muscle forces.

In conclusion, in the CMN model in the initial position, cervical muscles are represented by a number of straight line muscle elements that consist of several segments. The muscles curve around the vertebrae during neck bending. An overview of the modeled muscles can be found in the appendix. For more detailed information about the muscle model, the reader is referred to [15,21].

INITIAL POSITION - In reality, the neck muscles are slightly activated to maintain the initial position of the head. To incorporate this into the model would require neural excitation of the muscles utilizing a complex feedback mechanism. Since this is beyond the primary interest of this study, gravity is neglected to create an upright initial position of the head, and a simpler approach is used for muscle activation during impact.

MUSCLE ACTIVATION - As described above, it is assumed that the neck muscles are not activated at the time of impact. An increasing activation has been implemented in response to impact loading (see Figure 3). Muscular activation can be specified by mathematical modeling of neural feedback mechanisms [22]. However, the current musculoskeletal model was considered too complex for this approach. Instead it has been assumed that muscles are activated after a certain sensory threshold level has been exceeded ($t_{level}$ in Figure 3). Subsequently a neural reflex time $t_{reflex}$ is implemented as a pure delay. Thus the activation starts to rise at $t_{act}=t_{level}+t_{reflex}$ (see Figure 3). It takes about 55 ms after the moment of activation $t_{act}$ for the muscle active state to reach its maximum [b].

[b] Activation dynamics have been implemented as the step-response of two linear first-order systems in series, describing the excitation and activation dynamics with time constants of respectively 45 ms and 10 ms [23].

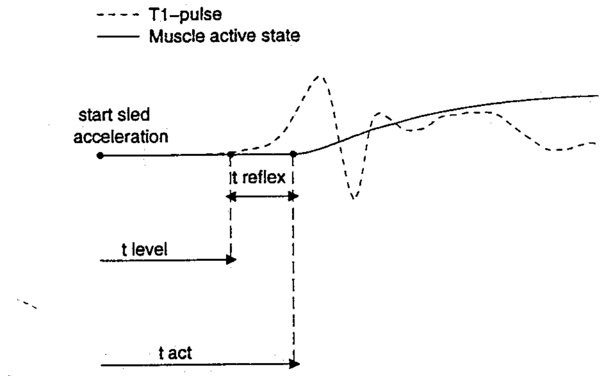


Figure 3: Active state of the muscles compared to the impact pulse for the head-neck. Activation starts at $t_{act} = t_{level} + t_{reflex}$.

Szabo *et al.* [14] hypothesize that muscle activity is triggered by lumbar spine acceleration. We assume that T1 acceleration could also be a trigger for muscle activation. Therefore, the sensory threshold in this study is based on a T1 acceleration level of 0.5g, resulting in a $t_{level}$ ranging from 45-62 ms. Reported motor reflex times range from 10-120 ms [13,14,24,25,26,27]. In the current study, a motor reflex delay of 25 ms ($t_{reflex}$) was chosen. After another 55 ms the muscle active state reaches its maximum[b], which in these simulations is 100% muscle activation. In a limited parametric study, the activation level and reflex times are varied to investigate their influence on the head-neck responses.

## RESPONSE TO VARIOUS IMPACTS

The model has been validated for frontal and lateral impact at several G levels using human volunteer responses [7,17]. The effect of muscle contraction on the head-neck response is studied by simulation with (active) and without (passive) muscle activation. The average horizontal acceleration in impact direction of vertebra T1 is used as input to the model to simulate the impact (see Figure 4). The corridors used to compare the model with are defined as the average volunteer response plus or minus the standard deviation [8]. Corridors are available for the linear and angular acceleration of the head's center of gravity relative to the laboratory coordinate system (+*x* is forward, +*y* is to the left, +*z* is upward); the trajectory of the occipital condyles and the center of gravity of the head relative to the T1-vertebral body; rotation of the head, which is the rotation of head center of gravity relative to T1; neck rotation, i.e. the neck link rotation relative to T1; head lag, which is neck rotation as a function of head rotation;

and neck link length. The neck link is defined as the straight line connecting T1 to the occipital condyles. As lower frontal impact levels have not yet been completely analyzed by the method described by Thunnissen *et al.* [8], only the resultant linear head acceleration, the angular acceleration, and the corrected peak value of the head and neck rotation are used.

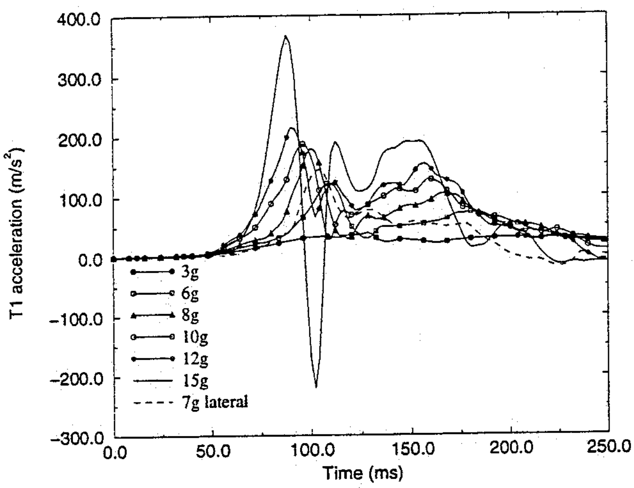


Figure 4: Average T1-acceleration used as input to the model to simulate the impact.

FRONTAL -15g - For the model with muscle activation, the extensor muscles are 100% activated to oppose the flexion motion of the head and neck. The results of the active CMN model and the active original model are compared in Figure 5[c] together with the response corridors of a frontal sled test with a sled acceleration of 15g. The head and neck rotation of the CMN model are reduced, as well as the displacements of the occipital condyles and center of gravity of the head. The head lag response shows that after a neck rotation of about 30 deg the head starts to rotate as well, and head and neck move more or less as one unit, which is also known as locking [6]. Overall, the response of the CMN model is improved and agrees adequately with the corridors.

The responses of the original and CMN model without muscle activation seem to be virtually identical. Since the muscles are the only difference between both models, it can be stated that with used muscle parameters, the influence of the passive behavior of the extra muscles is negligible. Examples of muscle force and muscle length are shown in the appendix.

Figure 6 compares the active response with the passive response of the CMN model. Muscle contraction clearly influences the response, as was already shown by De Jager [6] and Williams and Belytschko [9]. Head angular acceleration oscillates less for the active response due to muscle contraction. The trajectories of the occipital condyles and center of gravity of the head decrease significantly due to muscle contraction. Head rotation also shows a strong decrease in response, whereas neck rotation shows a smaller, but still significant reduction. Initially, the head lag for the active and passive response compare well.

Figure 7 depicts the intervertebral joint rotations for the active and passive response of the CMN model in comparison with static *in vivo* ranges of motion [15,28], as no ranges of motions during dynamic loading were available. Flexion occurs in all joints, except in the two upper joints, where extension initially takes place, illustrating that head rotation lags behind neck rotation. The C0-C1 rotation for the active response shows that the changes of rotation of the head relative to the neck are small after 125 ms, which confirms the observation regarding locking; that is, as mentioned before, rotation of the head relative to the neck is almost absent. The rotations of the four upper joints only slightly exceed the ranges of motions. Although reduced by muscle contraction, the rotations of C5-C6, C6-C7 and C7-T1 still seem to be unrealistically large.

LATERAL - 7g - Figure 8 shows the active and passive response of the CMN model and the response corridors for a 7g lateral sled test. For the model with muscle activation, the extensor and flexor muscles on the left side are 100% activated to oppose the motion of the head and neck to the right. All responses with active muscle behavior agree adequately with the corridors. Muscle contraction affects the head-neck motion strongly and causes the model responses to react sooner than the volunteer responses. Especially the trajectories and head *x*-rotation (lateral) are closer to the corridors. However, the *z*-rotation (axial), which already agreed with the corridor is hardly influenced by muscle activation. It can be observed from Figure 9 that all joint rotations for the active response lie within the static corridors [28], with the exception of the two lower joints that exceed the ranges of motion considerably. The muscle tensioning leads to smaller lateral joint rotations for all joints, however, the extension of the two upper cervical joints were found to increase.

FRONTAL - VARIOUS LEVELS - In Figures 10-14, the active (100%) and passive response to the 12g, 10g, 8g, 6g, and 3g impact simulations are shown in comparison with the human volunteer responses of the corresponding sled tests. As no experimental EMG data were available, the activation signal for the muscles is the same for all simulations. For these low and mid severity impacts, it is shown that the head and neck rotations are too large for the passive response, while they are too much restrained by maximum muscle contraction for the active response. Observed trends are that the response for linear and angular accelerations,

[c] Response characteristics are included at end of paper.

as well as the head and neck rotations, resemble the corridors better as the impacts become more severe.

PARAMETRIC STUDY MUSCLE ACTIVATION- A limited parametric study is performed by decreasing the muscle activation signal for frontal impact simulations. The model responses with 100% and 0% (passive) muscle activation are compared with the model responses with 25% and 50% activation. Figure 15 shows that a response to a 15g frontal impact with 100% muscle activation agrees well with the volunteer responses, whereas a 25% muscle activation provides promising results for a 3g frontal impact. It can be observed that the influence of the muscles increases with rising activation level. Similar trends were observed for the other frontal severities.

The simulations with a 25 ms reflex time are compared with different reflex times, i.e. 0 ms ,15 ms, and 50 ms, to investigate the influence of the time before muscles start to activate. Figure 16 shows that head and neck rotation are reduced by decreasing reflex times for the 15g and 3g frontal impact. These trends were also observed for the other frontal severities.

## DISCUSSION

In this study, the response of De Jager's detailed head-neck model is significantly improved by modeling the cervical musculature in more detail. The model consists of rigid head and vertebrae, linear viscoelastic discs, frictionless facet joints, nonlinear viscoelastic ligaments, and segmented contractile muscles. Human volunteer responses are used to validate the model. In contrast with former studies [6,9], the influence of muscle activity on the head-neck response is investigated by simulating with and without muscle activation and by varying the muscle activation level and reflex delay.

FRONTAL - 15g - The response of the active model is improved because the muscles are modeled in more detail and can curve around the vertebrae, which results in more realistic muscle lines of action in contrast with the original model. Head and neck motion is significantly reduced by muscle contraction. However, the head lag for the active and passive response are nearly identical. This is in contrast with observations made by Wismans *et al.* [29], who concluded from volunteer and Post Mortem Human Subject (PMHS) experiments that the muscles are responsible for the head lag and locking of head and neck rotation. It is more likely that the differences in head lag and locking are caused by different initial positions in volunteer and PMHS tests. In the current study the initial position is not varied. This could explain why the head lag and locking phenomena are almost identical for passive and active responses.

Although the muscles can curve around the vertebrae, in the CMN model extreme joint rotations still occur. Especially in the case of no muscle activation, this causes unrealistically large head and neck rotation. Thus, the neck response at the segmental level needs to be improved, which may be achieved by improving the characteristics of the intervertebral discs and ligamental structure.

LATERAL - 7g - Muscle contraction affects the head-neck motion strongly, which is also reflected by the frontal impact responses. The active model responses react sooner than the volunteer responses for the lateral impact. This could be caused by stiffening of the neck due to muscle contraction, which causes the neck to react sooner to an acceleration field. In the high severity lateral impact, the model with active muscle behavior agrees well with the volunteers for the linear and angular accelerations of the head, the trajectories of the occipital condyles, and center of gravity of the head and the head rotations.

FRONTAL - VARIOUS LEVELS - Muscle activation restrains the head and neck motion more with decreasing severities. A parametric study was performed in which the level of muscle activation was decreased. It can be concluded that the muscle activation level is very important for correctly describing the model response. Independent of the level of severity, the influence of the muscles increases with increasing muscle activation. Muscle contraction also increases with decreasing reflex delay. Thus, accurate muscle activation seems essential to control the human head-neck response to impacts. Therefore, muscle activation signal control patterns based on measurements of muscle activity (EMG) of volunteers during impact tests are needed.

It is possible that the volunteers, who were exposed to the impacts with an increasing order of severity, were more tensed during the high severity impacts because they were more aware and therefore more trained to reduce the effect of the impact. Therefore, the volunteer corridors for the low severity impacts probably represent volunteers who were more relaxed, or slightly tensed, while the corridors for the high severity impacts represent more tensed volunteers. This could explain why a maximum muscle activation with a reflex delay of 25 ms for a 15g frontal impact and a submaximum activation or a shorter muscle activation delay for a 3g frontal impact provides good results compared with the human volunteer corridors.

In all simulations, it can be observed that the active neck musculature plays a significant role in reducing head and neck rotation. However, the linear and angular accelerations are hardly influenced by muscle activation. This shows that validation of neck response in a human neck substitute on the basis of only head acceleration is insufficient.

To simplify the model, gravity was neglected, but for low severity impacts this will be a large amount of the acceleration field and, therefore, it should be taken into account. Thus, a new adaptation of the model is needed for the low severity impacts in which not only the muscle activation signal is improved, but the model should also include the gravitational force requiring an equilibrium in initial position of the head-neck system.

In the future we will focus on validating and improving the head-neck model for low severity rear-end impact conditions, because neck injuries often occur during these types of car accidents. However, the model should also be improved for other directions and severities. Not only muscle activation signals based on experiments, but also the neck response at segmental level will be required. Therefore, a study of human muscle behavior (EMG) and segmental neck kinematics during impact conditions is strongly recommended.

## SUMMARY AND CONCLUSIONS

- The detailed head-neck model by De Jager [6,15] has been improved by adapting the muscle geometry, including more muscles, and dividing the muscles into segments to enable muscle curvature. The CMN model comprises head and vertebrae, connected by intervertebral discs, ligaments, facet joints, and segmented Hill-type muscles.

- The model has been validated for high severity frontal and lateral impact with and without muscle activation. Responses with maximum muscle activation and a reflex time of 25 ms agreed well with the volunteer responses, especially due to introducing more realistic muscle lines of action.

- The model has also been verified for frontal impact at reduced G levels. The modeled muscles improved the active responses compared with the passive model. It can be concluded from this study that the amount of activation and the muscle motoric reflex delay is very important. Results indicate that a submaximum activation level or a larger reflex delay provides better results for the low severity impacts.

- Active muscle behavior seems essential to accurately describe the human head-neck response to impacts.

## REFERENCES


[1] Tien, C.S. and Huston, R.L.; Biodynamic modeling of the head/neck system. In *Field Accidents Data collection Analysis, Methodologies and Crash Injury Reconstruction*, pp 359-364, 1985, SAE special publication P-159, SAE Paper No. 850438.

[2] Deng, Y.C. and Goldsmith, W.; Response of a human head/neck/upper-torso replica to dynamic loading - II. analytical/numerical model. *Journal of Biomechanics*, 20:487-497, 1987.

[3] Happee, R. and Thunnissen, J.; Advances in human body modelling using MADYMO. In *Proceedings of the $5^{th}$ International Conference* MADYMO *User's Meeting*, FT. Lauderdale, 1994.

[4] Hill, A.V.; The heat of shortening and dynamic constants of muscles. In *Proceedings of Royal Society*, 126B, pp 135-195, 1938.

[5] Hill, A.V.; *First and Last Experiments in Muscle Mechanics.* Cambridge University Press, Cambridge, 1970.

[6] Jager, M. de, Sauren, A., Thunnissen, J. and Wismans, J.; A global and a detailed mathematical model for head-neck dynamics. In *Proceedings of the $40^{th}$ Stapp Car Crash Conference*, pp 269-281. Society of Automotive Engineers, 1996. SAE Paper No. 962430.

[7] Wismans, J., Oorschot, E. van, Woltring, H.J.; Omni-directional human head-neck response. In *Proceedings of the $30^{th}$ Stapp Car Crash Conference*, pp 313-331. Society of Automotive Engineers, 1986. SAE Paper No. 861893.

[8] Thunnissen, J.G.M., Wismans, J.S.H.M., Ewing, C.L. and Thomas, D.J.; Human volunteer head-neck response in frontal flexion: a new analysis. In *Proceedings of the $39^{th}$ Stapp Car Crash Conference*, pp 439-460. Society of Automotive Engineers, 1995. SAE Paper No. 952721.

[9] Williams, J.L. and Belytschko, J.T.; A three-dimensional model of the human cervical spine for impact simulation. *Journal of Biomedical Engineering*, 105:321-331, 1983.

[10] Mertz, H.; *The Kinematics and Kinetics of Whiplash.* PhD thesis, Wayne State University, 1967.

[11] Mertz, H.J. and Patrick, L.M.; Strength and response of the human neck. In *Proceedings of the $15^{th}$ Stapp Car Crash Conference*, pp 207-255. Society of Automotive Engineers, 1971. SAE Paper No. 710855.

[12] Schneider, L.W., Bowman, B.M., Snyder, R.G. and Peck, L.S.; A prediction of response of the head and neck of the U.S. adult military population to dynamic impact acceleration from selected dynamic test subjects, 12 month technical report UM-HSRI-76-10, University of Michigan, 1976.

[13] Foust, D.R., Chaffin, D.B., Snyder, R.G. and Baum, J.K.; Cervical range of motion and dynamic

response and strength of cervical muscles. In *Proceedings of the 17th Stapp Car Crash Conference*, pp 285-308. Society of Automotive Engineers, 1973. SAE Paper No. 730975.

[14] Szabo, T.J. and Welcher, J.B.; Human subject kinematics and electromyographic activity during low speed rear-end impacts. In *Proceedings of the 40th Stapp Car Crash Conference*, pages 295-315. Society of Automotive Engineers, 1996. SAE Paper No. 962432.

[15] Jager, M.K.J. de; *Mathematical Head-Neck Models for Acceleration Impacts*. PhD thesis, University of Eindhoven, 1996.

[16] Haaster, R. van; Modelling of the human head-neck system in impact conditions. Master's thesis, University of Eindhoven, 1996. WFW-report 96.107.

[17] Ewing, C.L. and Thomas, D.J.; Human head and neck response to impact acceleration. Monograph 21 USAARL 73-1, Naval Aerospace and Regional Medical Centre, Pensacola, 1972.

[18] TNO Crash-Safety Research Centre, Delft, The Netherlands. *MADYMO Update, Version 5.2.1*, 1997.

[19] Happee, R. and Thunnissen, J.G.M.; The role of muscular dynamics in impact conditions, simulation of neck behavior in frontal impact. TNO-report 94.OR.BV.047.1/RHA, TNO Crash-Safety Research Centre, Delft, The Netherlands, 1994.

[20] Seirig, A. and Arvikar R.J.; *Biomechanical Analysis of the Musculoskeletal Structure for Medicine and Sports*. Hemisphere Publishing Corporation, New York, NY, 1989.

[21] TNO Crash-Safety Research Centre, Delft, The Netherlands. *MADYMO Theory Manual, Version 5.2*, 1996.

[22] Pape, K.; Regulatory functions of the cervical muscle system, simulation of neck behaviour under impact conditions. Master's thesis. University of Eindhoven, 1995. WFW-report 95.106.

[23] Winters, J.M. and Stark, L.; Analysis of fundamental human movement patterns through the use of in-depth antagonistic muscle models. *IEEE Transactions on Biomedical Engineering*. BME-32-10: 826-839, 1989.

[24] Schneider, L.W., Foust, D.R., Bowman, B.M., Snyder, R.G., Chaffin, D. B. Abdelnour, T.A. and Baum, J.K.; Biomechanical properties of the human neck in lateral flexion. In *Proceedings of the 19th Stapp Car Crash Conference*, pp 455-485. Society of Automotive Engineers, 1975. SAE Paper No. 751156.

[25] Tennyson, S.A., Mital, N.K. and King, A.I.; Electromyographic signals of the spinal musculature during +Gz impact acceleration. *Orthopedic Clinics of North America*, 8:97-119, 1977.

[26] Reid, S.E., Raviv, G. and Reid, S.E. Jr.; Neck muscle resistance to head impact. *Aviation, Space, and Environmental Medicine*, pp 78-84, 1981.

[27] Colebatch, J.G., Halmagyi, G.M. and Skuse, N.F.; Myogenic potentials generated by a click-evoked vestibulocollic reflex. *Journal of Biomechanics*, 18:167-176, 1994.

[28] White III, A.A. and Panjabi, M.M.; *Clinical Biomechanics of the Spine*. J.B. Lippincott Company, 2nd edition, 1990.

[29] Wismans, J., Philippens, M., Oorschot, E. van, Kallieris, D. and Mattern, R; Comparison of human volunteer and cadaver head-neck response in frontal flexion. In *Proceedings of the 31th Stapp Car Crash Conference*, Society of Automotive Engineers, 1987. SAE Paper No. 872194.

[30] Yamaguchi, G.T., Sawa, A.G.U., Moran, D.W., Fessler, M.J. and Winters, J.M.; A survey of human musculotendon actuator parameters. In *Multiple Muscles Systems: Biomechanics and Movement Organisation*, edited by Winters, W.M. and Woo, S.L.Y., Springer-Verlag, 1990.

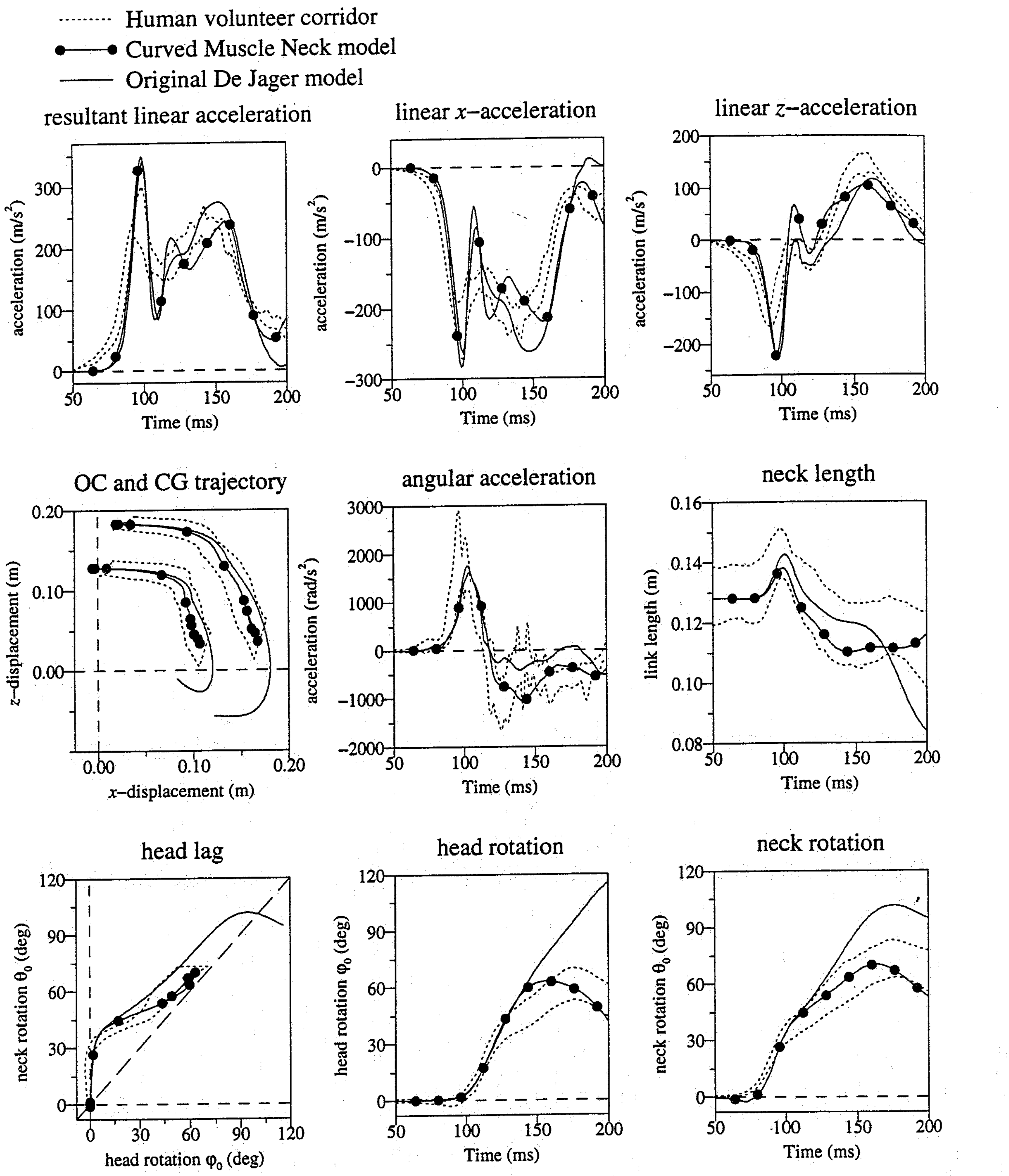


Figure 5: Response to 15g frontal impact of the original and CMN model with maximum active muscle behavior compared with human volunteer response corridors. +*x* is forward, +*z* is upward. Accelerations are at the head's center of gravity.

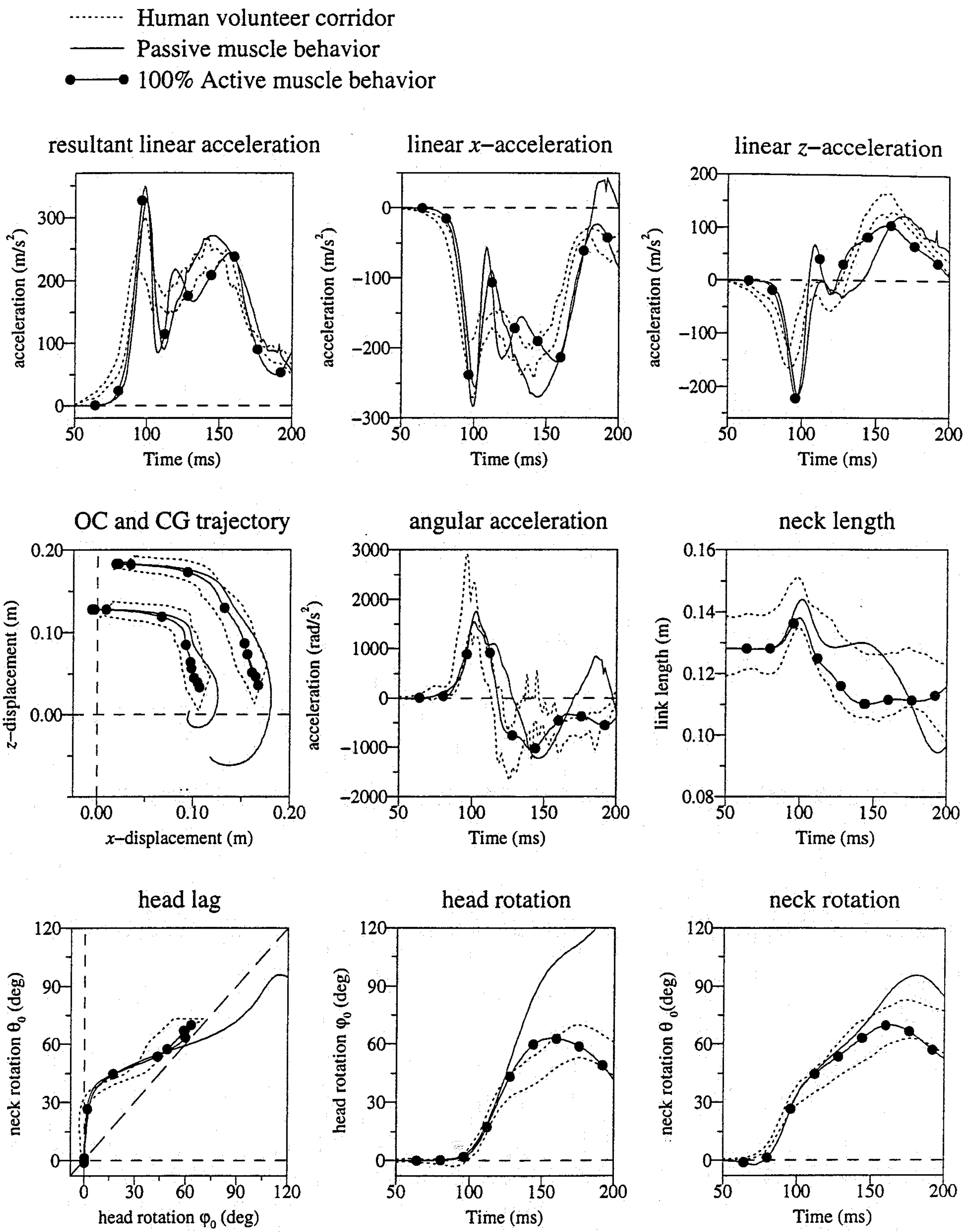


Figure 6: Response to 15g frontal impact of the CMN model with passive and maximum active muscle behavior compared with human volunteer response corridors. $+x$ is forward, $+z$ is upward. Accelerations are at the head's center of gravity.

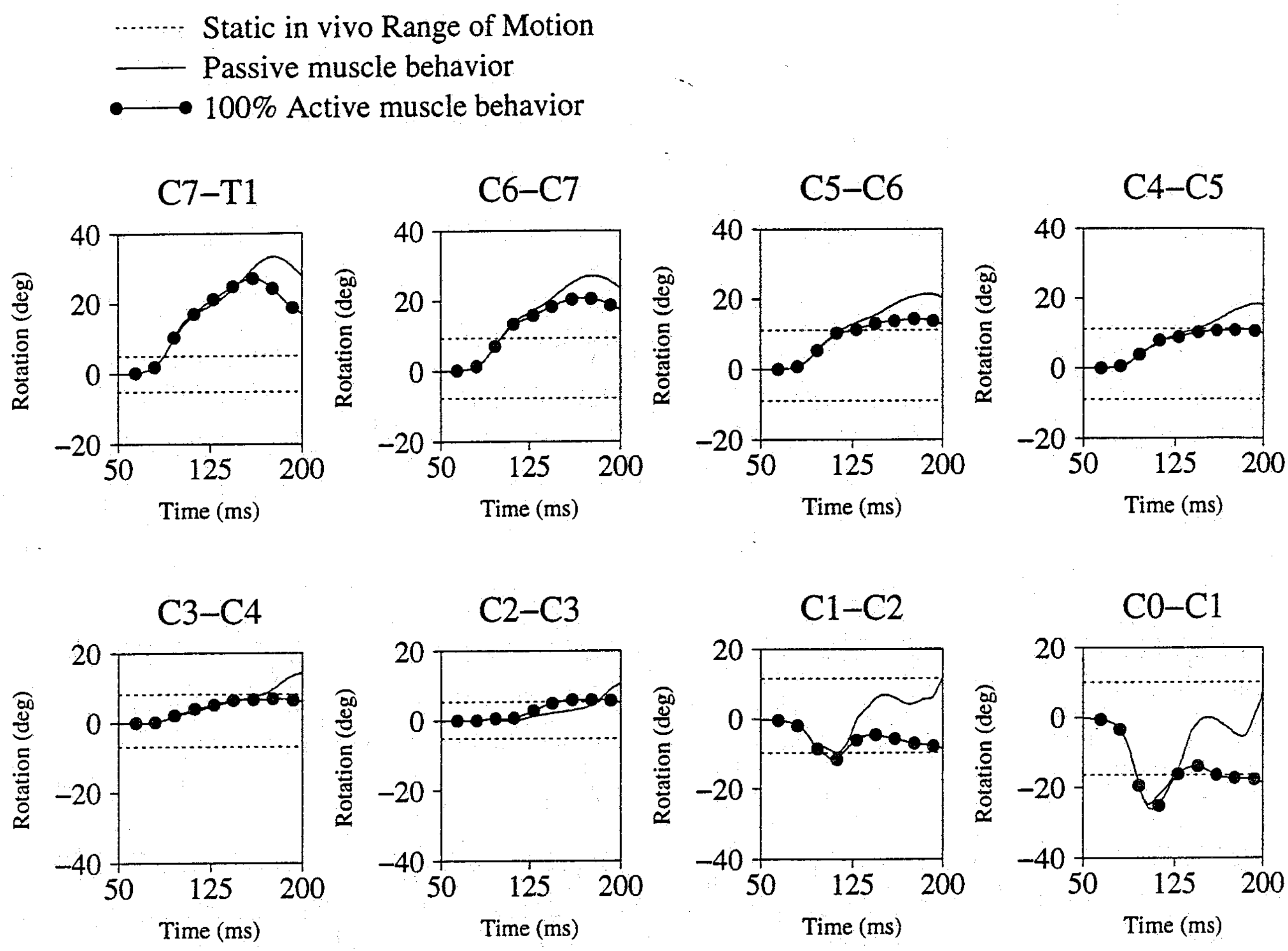


Figure 7: Flexion/extension (y-rotation) of the intervertebral joints for the CMN model with passive and maximum acti muscle behavior for the 15g frontal impact compared with static *in vivo* ranges of motion [15, 28].

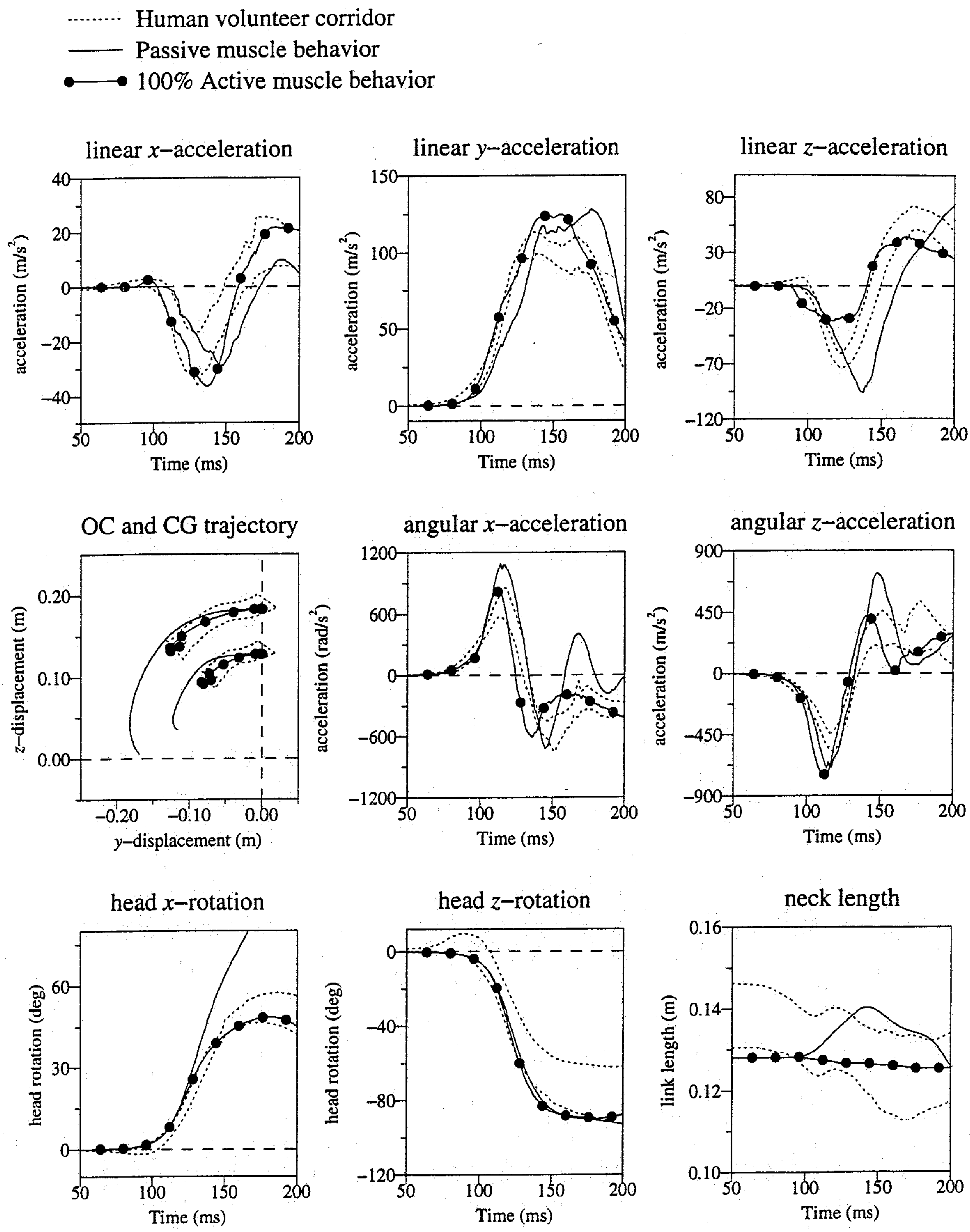


Figure 8: Response to 7g lateral impact of the CMN model with passive and maximum active muscle behavior compared with human volunteer response corridors. +*x* is forward, +*z* is upward. Accelerations are at the head's center of gravity.

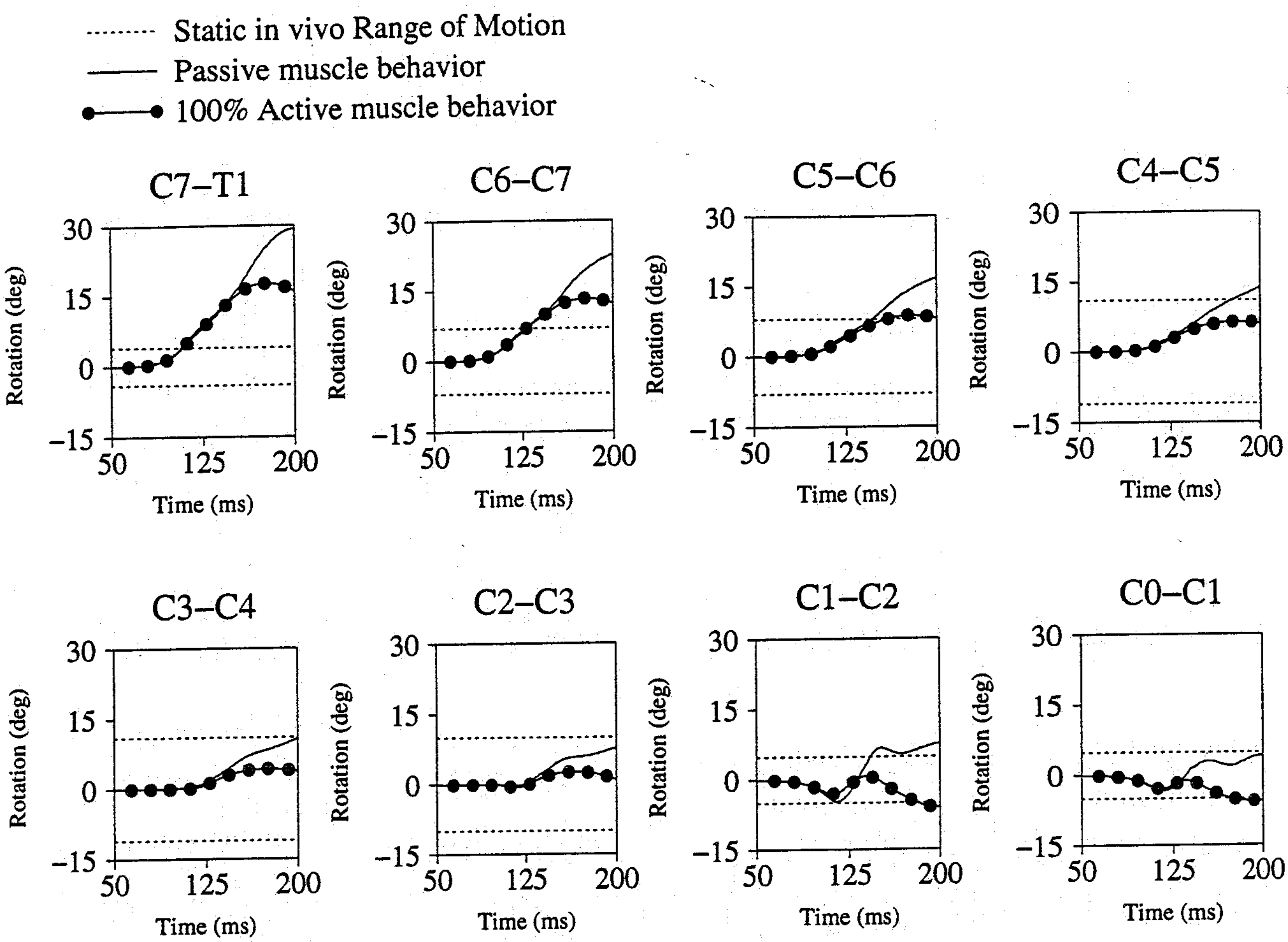


Figure 9: Lateral bending (*x*-rotation) of the intervertebral joints for the CMN model with passive and maximum active muscle behavior for the 7g lateral impact compared with static *in vivo* ranges of motion [15, 28].

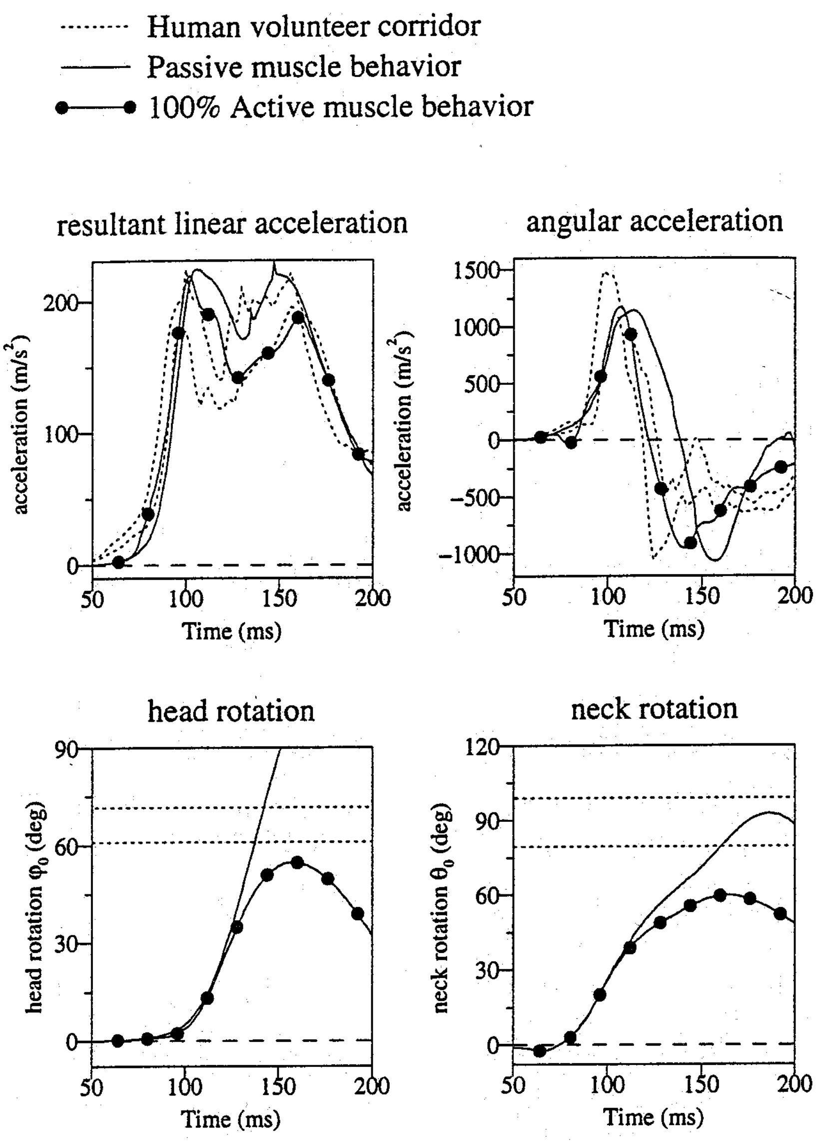


igure 10: Response to 12g frontal impact of the CMN model with passive and maximum active muscle behavior compared with human volunteer response corridors. Accelerations are at the head's center of gravity.

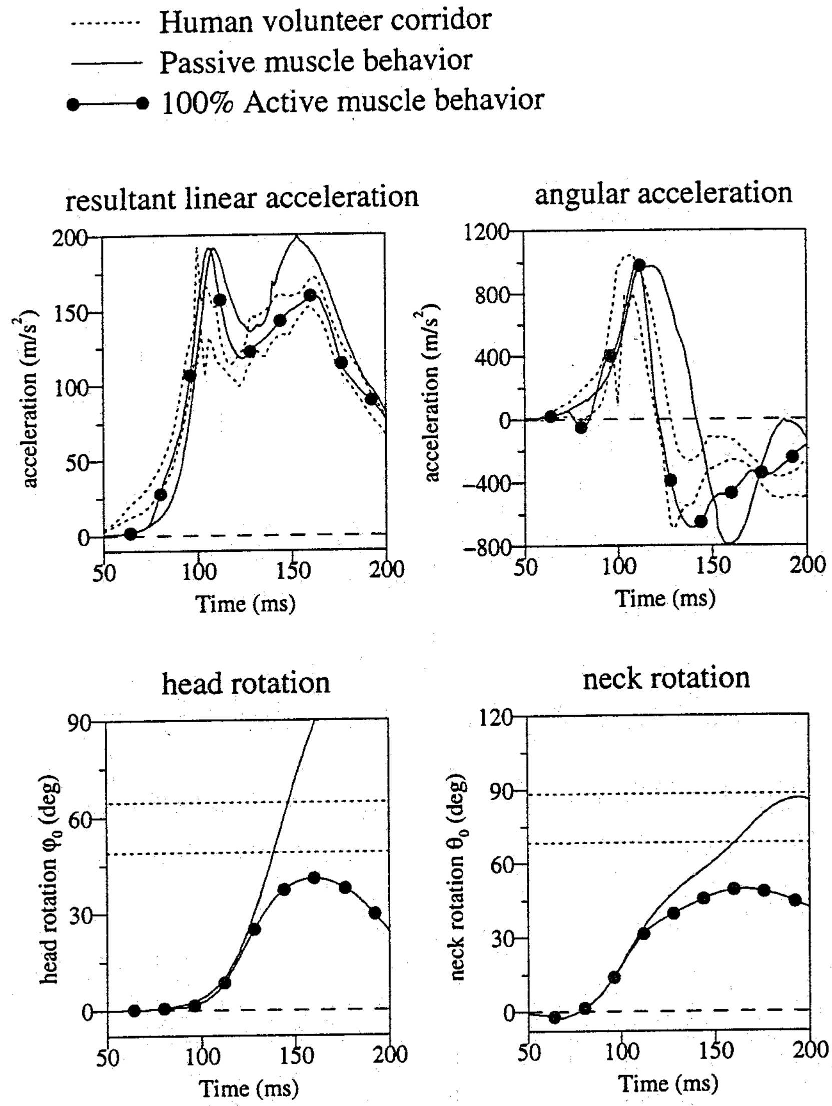


Figure 11: Response to 10g frontal impact of the CMN model with passive and maximum active muscle beh[avior] compared with human volunteer response corridors. Accelerations are at the head's center of gravity.

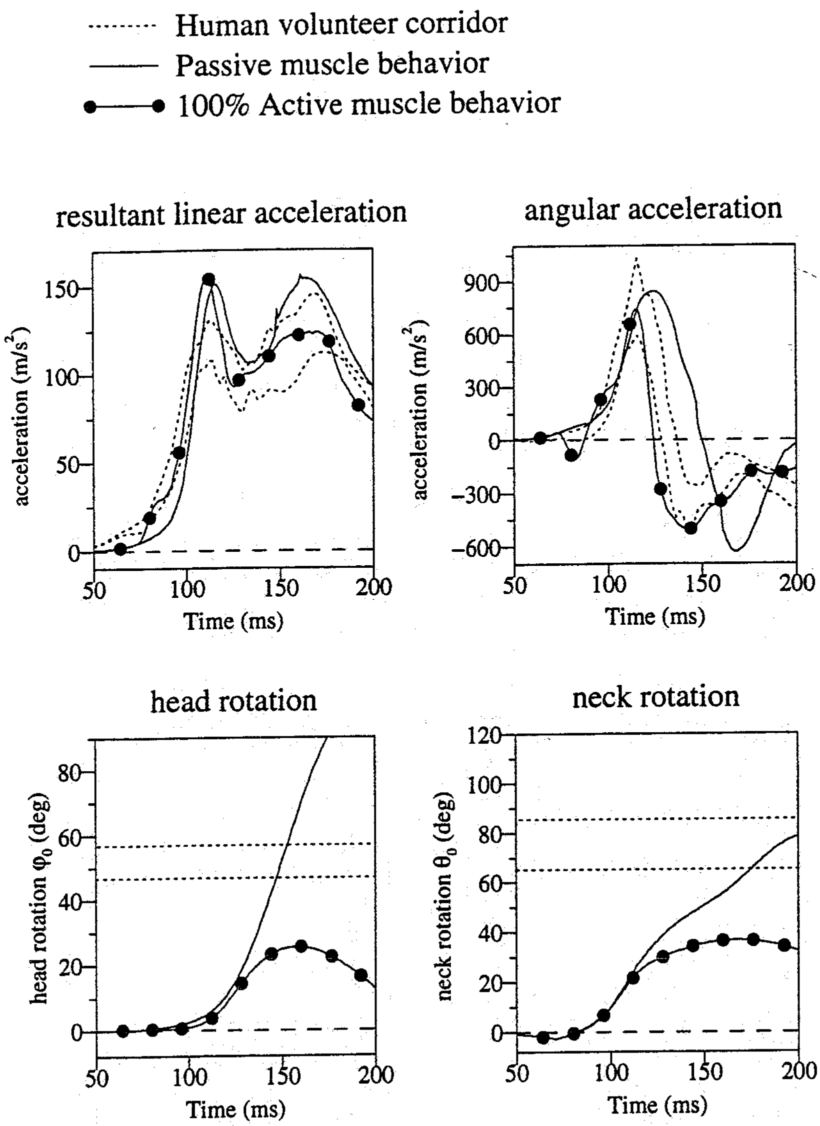


ure 12: Response to 8g frontal impact of the CMN model with passive and maximum active muscle behavior compared h human volunteer response corridors. Accelerations are at the head's center of gravity.

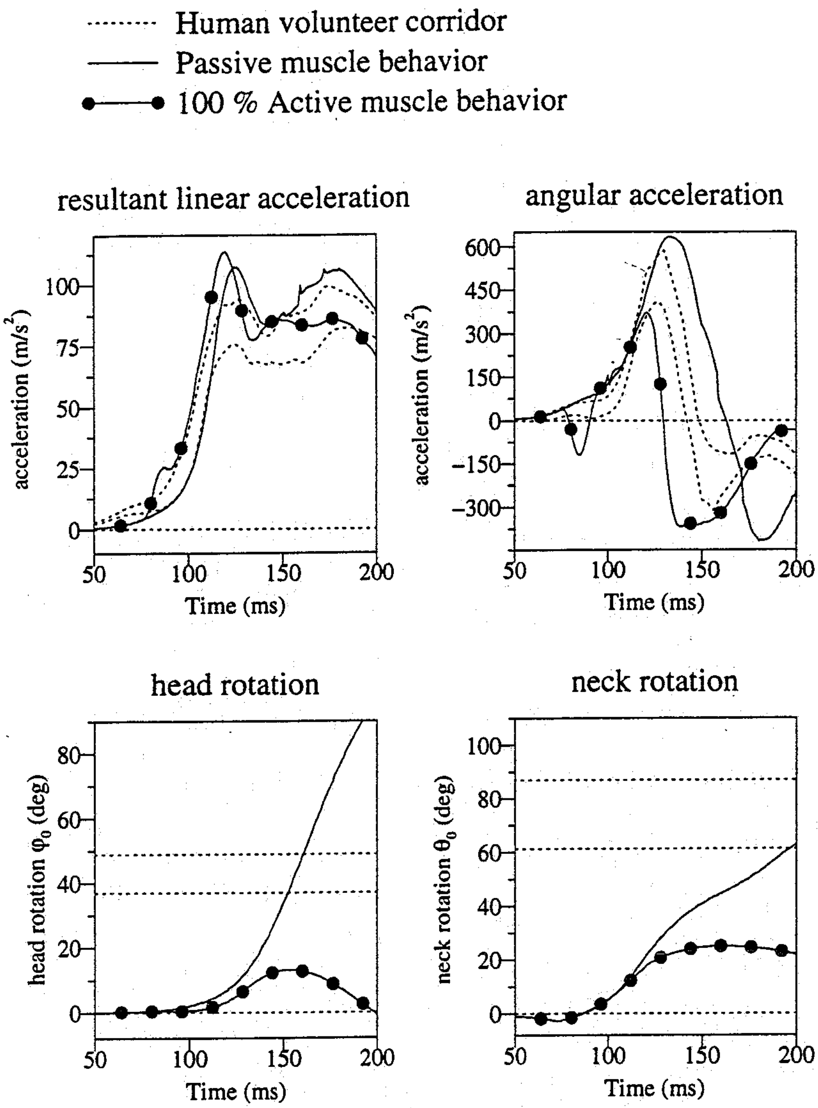


Figure 13: Response to 6g frontal impact of the CMN model with passive and maximum active muscle behavior comp
with human volunteer response corridors. Accelerations are at the head's center of gravity.

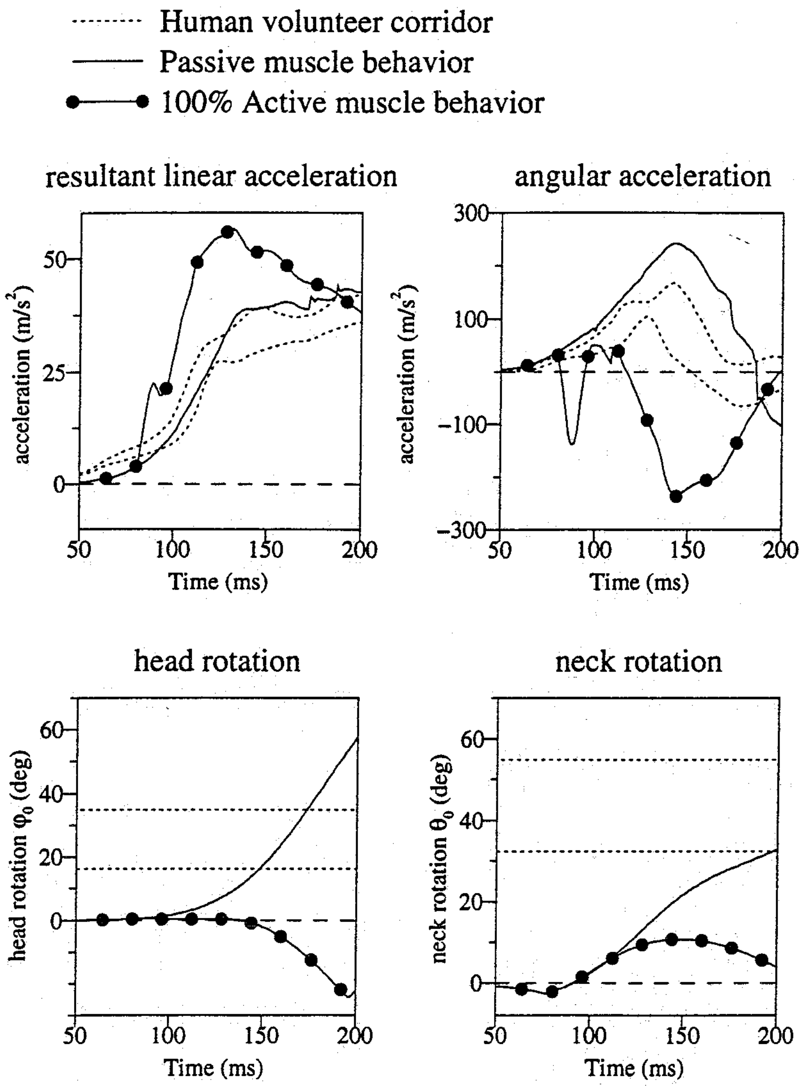


Figure 14: Response to 3g frontal impact of the CMN model with passive and maximum active muscle behavior compared with human volunteer response corridors. Accelerations are at the head's center of gravity.

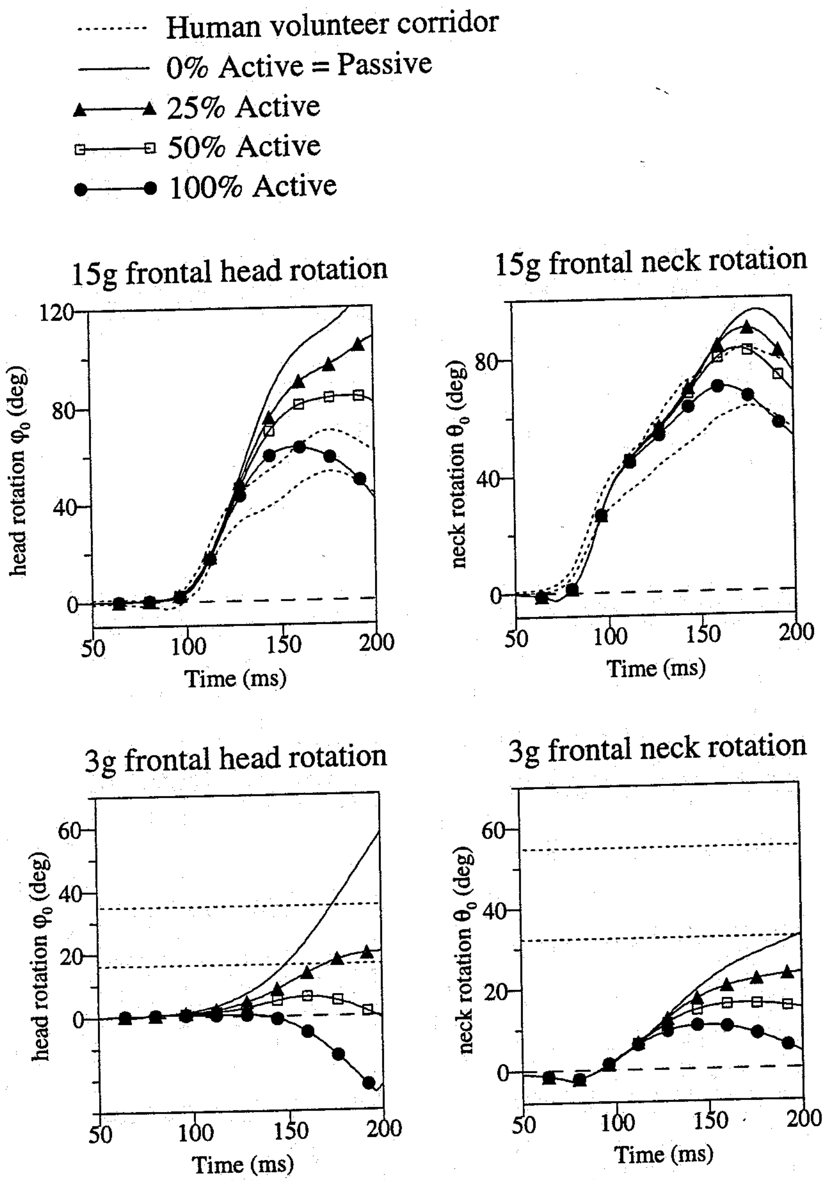


Figure 15: Head and neck response to 15g and 3g frontal impact of the CMN model with muscle activation at differ levels compared with human volunteer response corridors. Accelerations are at the head's center of gravity.

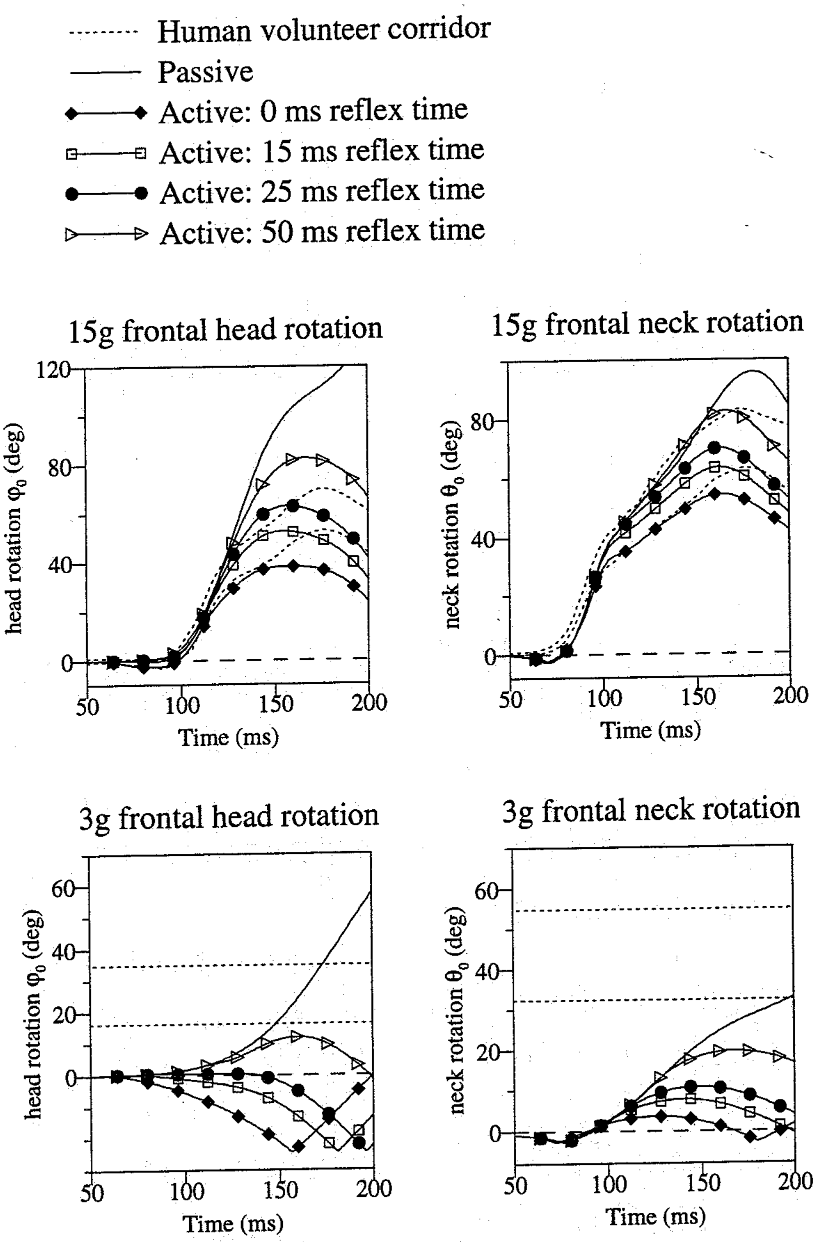


Figure 16: Head and neck response to 15g and 3g frontal impact of the CMN model with different reflex times for muscle activation compared with human volunteer response corridors. Accelerations are at the head's center of gravity.

## APPENDIX

The muscle model describes the Contractile Element (CE) and the Parallel Element (PE) of a Hill model. It describes the tension force $F$ as a function of its length $l$, lengthening velocity $v$, and the active state $A$. Passive muscle behavior is modeled similar to the model of Deng and Goldsmith [2] by a nonlinear force-strain relation [15]. Active muscle behavior is modeled using the standard functions provided by MADYMO [21]. The parameters for the Hill muscle model of the current head-neck system have been chosen according to Happee and Thunnissen [19], who extensively studied the available literature. These parameters and the general material parameters are included in Table A.2.

Examples of muscle force and normalized muscle length are plotted against the time in Figure A1 and A2. The resultant forces of the muscles during the passive simulation are very small and therefore not shown.

The muscles used are included in Table A.1. To resemble the anatomy of the human muscles, the muscles in the model are divided into several elements [20], while each element is divided into segments so the muscles can curve around the vertebrae. The intermediate sliding points are located on the points of intersection of the muscle line of action in initial position and the $xy$-plane of the intermediate vertebrae. The sum of the physical cross-sectional areas (PCSAs) of the muscle elements is equal to the human muscle PCSA according to De Jager [15] and Yamaguchi [30], or determined from MRI pictures [16].

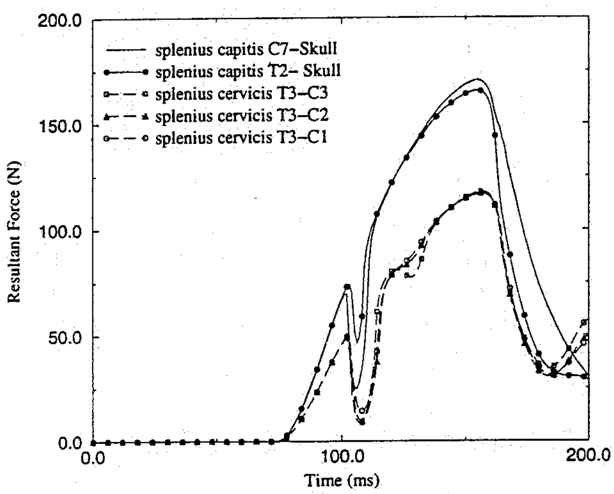


Figure A1: Force-time curve of a neck muscle for the 15g frontal impact with 100 % muscle activation and $t_{reflex}$= 25 ms.

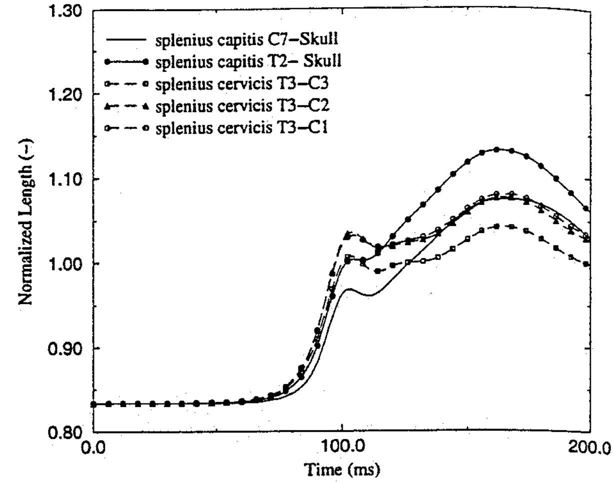


Figure A2: Normalized length-time curve of a neck muscle for the 15g frontal impact with 100 % muscle activation and $t_{reflex}$= 25 ms.

Table A.1a Flexor muscles in the CMN model.

| Flexor muscle[d] | Origin | Insertion | PCSA $[cm^2]$ |
|---|---|---|---|
| longus colli | T1 | C6 | 0.12 |
| longus colli | T1 | C5 | 0.12 |
| longus colli | T1 | C4 | 0.12 |
| longus colli | T1 | C3 | 0.12 |
| longus colli | T1 | C2 | 0.12 |
| longus colli | T1 | C1 | 0.12 |
| longus colli | T1 | Skull | 0.12 |
| longus capitis | C3 | Skull | 0.25 |
| longus capitis | C4 | Skull | 0.25 |
| longus capitis | C5 | Skull | 0.25 |
| longus capitis | C6 | Skull | 0.25 |
| scalenus anterior[e] | T1 | C4 | 0.9 |
| scalenus medius[e] | T1 | C3 | 1.0 |
| scalenus posterior[e] | T1 | C5 | 0.9 |
| lumped hyoids[f] | T1 | Skull | 3.0 |

[d] modified compared to De Jager model
[e] not changed compared to De Jager model
[f] new compared to De Jager model

Table A.1b Extensor muscles in the CMN model.

| Extensor muscle[d] | Origin | Insertion | PCSA [$cm^2$] |
|---|---|---|---|
| trapezius[e] | T1 | Skull | 1.8 |
| sternocleidomastoid[e] | T1 | Skull | 3.7 |
| splenius capitis | C7 | Skull | 1.55 |
| splenius capitis | T2 | Skull | 1.55 |
| splenius cervicis | T3 | C3 | 1.05 |
| splenius cervicis | T3 | C2 | 1.05 |
| splenius cervicis | T3 | C1 | 1.05 |
| semispinalis capitis | C4 | Skull | 0.7 |
| semispinalis capitis | C5 | Skull | 0.7 |
| semispinalis capitis | C6 | Skull | 0.7 |
| semispinalis capitis | C7 | Skull | 0.7 |
| semispinalis capitis | T3 | Skull | 0.7 |
| semispinalis cervicis | T1 | C2 | 0.11 |
| semispinalis cervicis | T2 | C3 | 0.22 |
| semispinalis cervicis | T3 | C4 | 0.33 |
| semispinalis cervicis | T4 | C5 | 0.44 |
| semispinalis cervicis | T5 | C6 | 0.55 |
| semispinalis cervicis | T6 | C7 | 0.66 |
| longissimus capitis | C3 | Skull | 0.083 |
| longissimus capitis | C4 | Skull | 0.083 |
| longissimus capitis | C5 | Skull | 0.083 |
| longissimus capitis | C6 | Skull | 0.083 |
| longissimus capitis | C7 | Skull | 0.083 |
| longissimus capitis | T2 | Skull | 0.083 |
| longissimus cervicis | T2 | C2 | 0.12 |
| longissimus cervicis | T2 | C3 | 0.12 |
| longissimus cervicis | T2 | C4 | 0.12 |
| longissimus cervicis | T2 | C5 | 0.12 |
| longissimus cervicis | T2 | C6 | 0.12 |
| longissimus cervicis | T2 | C7 | 0.12 |
| levator scapulae[f] | Scapula | C1 | 0.25 |
| levator scapulae[f] | Scapula | C2 | 0.25 |
| levator scapulae[f] | Scapula | C3 | 0.25 |
| levator scapulae[f] | Scapula | C4 | 0.25 |
| multifidus cervicis[f] | C5 | C2 | 0.2 |
| multifidus cervicis[f] | C6 | C2 | 0.2 |
| multifidus cervicis[f] | C6 | C3 | 0.2 |
| multifidus cervicis[f] | C7 | C3 | 0.2 |
| multifidus cervicis[f] | C7 | C4 | 0.2 |
| multifidus cervicis[f] | T1 | C4 | 0.2 |
| multifidus cervicis[f] | T1 | C5 | 0.2 |
| multifidus cervicis[f] | T2 | C5 | 0.2 |
| multifidus cervicis[f] | T2 | C6 | 0.2 |
| multifidus cervicis[f] | T3 | C6 | 0.2 |
| multifidus cervicis[f] | T3 | C7 | 1.0 |
| multifidus cervicis[f] | T4 | C7 | 1.2 |

Table A.2 Muscle parameters

| Description | Parameter | Value or formula |
|---|---|---|
| physiological cross-sectional area | PCSA [$m^2$] | see Table A.1 |
| maximum isometric stress | $\sigma_{max}$ [$N*m^{-2}$] | 1E6 |
| CE rest length | $l_{ce0}$ [m] | dependent on initial position of muscle |
| CE maximum relative shortening velocity | $V_{maxr}$ [$s^{-1}$] | 5 |
| maximum isometric force | $F_{max}$ [N] | $\sigma_{max}$ *PCSA |
| CE optimum length=PE rest length | $l_{opt}=l_{ref}$ [m] | 1.2* $l_{ce0}$ |
| CE maximum shortening velocity | $V_{max}$ [$m*s^{-1}$] | $V_{maxr}$ * $l_{opt}$ = 0.6 |
| CE velocity shape parameter | $Ce_{sh}$ [ ] | 0.5 |
| CE velocity shape parameter lengthening | $CE_{shl}$ [ ] | 0.05 |
| CE maximum relative force | $CE_{ml}$ [ ] | 1.5 |
| CE force-length parameter | $S_k$ [ ] | 0.54 |
| PE strain with $F_{PE}=F_{max}$ | $PE_{xm}$ [ ] | 0.8 |
| PE shape parameter | $PE_{sh}$ [ ] | 10 |
| time-constant increasing active state | $\tau_{ac}$ [ms] | 10 |
| time-constant decreasing active state | $\tau_{da}$ [ms] | 40 |
| time-constant neural excitation | $\tau_{ne}$ [ms] | 45 |